

Stability Margins of Neural Network Controllers*

Neelay Junnarkar¹, Murat Arcak¹, and Peter Seiler²

Abstract—We present a method to train neural network controllers with guaranteed stability margins. The method is applicable to linear time-invariant plants interconnected with uncertainties and nonlinearities that are described by integral quadratic constraints. The type of stability margin we consider is the disk margin. Our training method alternates between a training step to maximize reward and a stability margin-enforcing step. In the stability margin enforcing-step, we solve a semidefinite program to project the controller into the set of controllers for which we can certify the desired disk margin.

I. INTRODUCTION

Neural network controllers trained through standard learning techniques show promise to overcome limitations of traditional control designs, but provide no guarantees on closed-loop behavior. This has limited the use of neural networks in safety-critical applications, such as aerospace, where it is common for regulatory agencies to formulate controller robustness requirements in terms of stability margins, such as classical gain and phase margins [1].

Recent work on safe learning has focused on verification and synthesis of neural network controllers. References [2]–[4] verify asymptotic stability and find inner approximations to regions of attraction of feedback systems involving neural networks. Methods that synthesize neural network controllers and jointly certify closed-loop stability include [5]–[8]. These methods differ in the types of plants considered, with [6] considering linear time-invariant (LTI) plants, [7] addressing LTI plants with sector-bounded uncertainties, and [5], [8] studying LTI plants interconnected with uncertain blocks described by integral quadratic constraints.

Besides being used as controllers, neural networks have also been explored as system models. Reference [9] uses linear matrix inequality techniques to analyze stability of an equilibrium of a recurrent neural network. Reference [10] analyzes approximation capabilities, controllability, and observability of recurrent neural networks. These results can be used for verifying closed-loop properties of a neural network controller by modeling the interconnection of the controller and plant as a neural network. However, they are less amenable to neural network controller synthesis due to the structure imposed by the fixed plant parameters.

In safety-critical applications, such as aviation, the classical notions of gain and phase margins are well-accepted

to the point of being a part of regulations of the Federal Aviation Administration [1]. Satisfaction of a stability margin ensures the controller will stabilize a plant despite a class of unmodeled dynamics. However, it is possible for systems with large gain and phase margins to be destabilized by an arbitrarily small simultaneous variation in plant gain and phase [11]. Instead, the notion of *disk margin* [12] allows simultaneous gain and phase variations. Although the disk margin accounts for LTI uncertainty described in the frequency domain, it can be reinterpreted in the time domain and generalized to nonlinear and time-varying plant and controller models. This has been used in [13] to assess disk margins of linear parameter-varying feedback systems.

In this paper, we present a method to train a neural network controller to maximize a reward subject to guaranteed disk margins. We leverage integral quadratic constraints to describe the disk margin and the neural network activation functions in time domain. We derive linear matrix inequality conditions for Lyapunov stability and translate them to semidefinite programs that enforce stability margins after each training step in the reinforcement learning process. A neural network trained through this method can be used in place of a traditional controller when stability margins are required. This allows improving an auxiliary performance metric, used as the reward in training, while satisfying the same robustness constraints as the traditional controller.

In Section II, we provide background on disk margins and our neural network model, and provide the problem statement. In Section III, we characterize the disk margin of the closed-loop system with a neural network controller. In Section IV, we present a method to train a neural network controller to maximize reward subject to the closed-loop satisfying a disk margin. In Section V, we demonstrate our method in simulation for a flexible rod on a cart.

A. Notation

$\mathbb{R}_{\geq 0}$ denotes the set of nonnegative real numbers, \mathcal{L}_2^n the space of square-integrable functions from $\mathbb{R}_{\geq 0}$ to \mathbb{R}^n , and \mathcal{L}_{2e}^n the space of functions from $\mathbb{R}_{\geq 0}$ to \mathbb{R}^n that are square-integrable on $[0, T]$ for all $T > 0$. We drop the superscript for the dimension of the codomain when clear from context. We use $(\star)^\top X y$ to denote $y^\top X y$, and $\text{He}(y)$ to denote $y + y^\top$.

II. BACKGROUND AND PROBLEM SETUP

We consider the problem of robustly stabilizing a plant using a neural network controller, with the further objective of maximizing a reward. We first describe the plant uncertainty and neural network, and then give the problem formulation.

arXiv:2409.09184v1 [eess.SY] 13 Sep 2024

*Supported by NFS CNS-2111688 and AFOSR FA9550-23-1-0732.

¹Neelay Junnarkar and Murat Arcak are with the Department of Electrical Engineering and Computer Science, University of California, Berkeley, CA 94720 USA (neelay.junnarkar@berkeley.edu, arcak@berkeley.edu)

²Peter Seiler is with the Department of Electrical Engineering and Computer Science, University of Michigan, Ann Arbor, MI 48109 USA (pseiler@umich.edu)

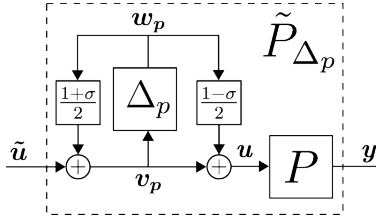


Fig. 1. Block-diagram of disk margin uncertainty at plant input.

A. Plant Model and Disk Margins

Consider the nominal plant, P :

$$\begin{bmatrix} \dot{x}_p(t) \\ y(t) \end{bmatrix} = \begin{bmatrix} A_p & B_p \\ C_p & 0 \end{bmatrix} \begin{bmatrix} x_p(t) \\ u(t) \end{bmatrix} \quad (1)$$

where $x_p(t) \in \mathbb{R}^{n_p}$, $y(t) \in \mathbb{R}^{n_y}$, $u(t) \in \mathbb{R}^{n_u}$ are the plant state and output, and control input at time t . Although we study a LTI plant for brevity, the results extend to plants with nonlinearities described by integral quadratic constraints.

We describe robustness to uncertainty with a disk margin. The traditional disk margin $D(\alpha, \sigma)$ accounts for LTI input uncertainty whose frequency response, in each channel, lies in the disk parameterized by $\alpha \in \mathbb{R}_{\geq 0}$ and $\sigma \in \mathbb{R}$:

$$\left\{ \frac{1 + \frac{1-\sigma}{2}\delta}{1 - \frac{1+\sigma}{2}\delta} : \delta \in \mathbb{C} \text{ with } |\delta| < \alpha \right\}.$$

The value α determines the size of the uncertainty disk. Note that the disk margin can be used to compute lower bounds on the classical gain and phase margins. For example, if the system remains stable for $D(\alpha, \sigma)$, then the system is stable for all gain variations in the range $[\gamma_{\min}, \gamma_{\max}]$ where

$$\gamma_{\min} = \frac{2 - \alpha(1 - \sigma)}{2 + \alpha(1 + \sigma)} \text{ and } \gamma_{\max} = \frac{2 + \alpha(1 - \sigma)}{2 - \alpha(1 + \sigma)}.$$

The disk margin definition above can be interpreted as robustness to input unmodeled dynamics described by the class of transfer functions

$$H_{\Delta_p}(s) = \left(I + \frac{1-\sigma}{2} \Delta_p(s) \right) \left(I + \frac{1+\sigma}{2} \Delta_p(s) \right)^{-1}$$

where Δ_p is LTI, diagonal, and $\|\Delta_p\|_{\mathcal{H}_\infty} < \alpha$. The choice $\Delta_p(s) = 0$ gives $H_{\Delta_p}(s) = I$, which corresponds to the nominal system. The input uncertainty $H_{\Delta_p}(s)$ is represented in block-diagram form in Figure 1, where

$$\begin{aligned} y &= Pu, & u &= v_p + \frac{1-\sigma}{2} w_p, \\ v_p &= \tilde{u} + \frac{1+\sigma}{2} w_p, & w_p &= \Delta_p v_p. \end{aligned} \quad (2)$$

The uncertain system from input \tilde{u} to output y , for a particular Δ_p , is denoted by \tilde{P}_{Δ_p} .

This interpretation allows us to broaden the disk margin to non-LTI uncertainty by generalizing Δ_p to be \mathcal{L}_2 norm-bounded by α . The class of plants which must be stabilized is then $\mathcal{M}_\alpha = \{\tilde{P}_{\Delta_p} \mid \mathcal{L}_2 \text{ gain of } \Delta_p \text{ is } < \alpha\}$. In the rest of this paper, we say that a controller satisfies the disk margin $D(\alpha, \sigma)$ if it stabilizes the class of plants \mathcal{M}_α .

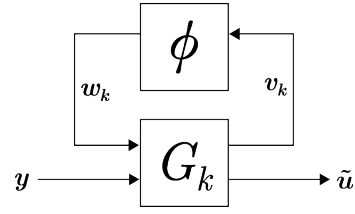


Fig. 2. The neural network controller is modeled as the interconnection of an LTI system G_k and activation functions ϕ .

B. Neural Network Controller Model

We model the neural network controller as the interconnection of an LTI system and activation functions (Figure 2):

$$\begin{bmatrix} \dot{x}_k(t) \\ v_k(t) \\ \tilde{u}(t) \end{bmatrix} = \begin{bmatrix} A_k & B_{kw} & B_{ky} \\ C_{kv} & D_{kvw} & D_{kvy} \\ C_{ku} & D_{kuw} & D_{kuy} \end{bmatrix} \begin{bmatrix} x_k(t) \\ w_k(t) \\ y(t) \end{bmatrix}, \quad (3)$$

$$w_k(t) = \phi(v_k(t)),$$

where $x_k(t) \in \mathbb{R}^{n_k}$, $v_k(t) \in \mathbb{R}^{n_\phi}$, and $w_k(t) \in \mathbb{R}^{n_\phi}$ are, respectively, the controller state, the input to the activation function ϕ , and the output of the activation function ϕ at time t . Many neural networks can be modeled in this form, though we restrict ourselves to neural networks without biases to ensure that the controller does not shift the equilibrium.

The activation function ϕ is memoryless and applied elementwise: $w_{k,i} = \phi_i(v_{k,i})$. Each scalar activation function ϕ_i is sector-bounded in $[0, 1]$, and slope-restricted in $[0, 1]$. Common activation functions that satisfy the sector bounds and slope restrictions are tanh and ReLU.

The controller (3) is well-posed if there exists a unique solution for w_k in the implicit equation $w_k = \phi(C_{kv}x_k + D_{kvw}w_k + D_{kvy}y_k)$ for all x_k and y_k . The system is trivially well-posed if $D_{kvw} = 0$ but otherwise requires constraints on D_{kvw} . We refer to [8] for a discussion of this issue.

When $n_k = 0$, this controller model simplifies to $\tilde{u}(t) = D_{kuw}w_k(t) + D_{kuy}y(t)$ where $w_k(t) = \phi(D_{kvw}w_k(t) + D_{kvy}y(t))$. This is a static implicit neural network (INN), which encompasses common classes of neural networks, including fully connected feedforward networks, convolutional layers, max-pooling layers, and residual networks [14].

For example, consider the feedforward neural network:

$$\tilde{u} = W_L w_L + b_L, w_{l+1} = \phi_l(W_l w_l + b_l), w_0 = y.$$

With $w_k = [w_1 \ \dots \ w_L]^\top$ and $\phi = [\phi_0 \ \dots \ \phi_{L-1}]^\top$, this can be represented by the following INN:

$$\tilde{u} = \underbrace{\begin{bmatrix} 0 & \dots & 0 & W_L \end{bmatrix}}_{D_{kuw}} w_k + \underbrace{\begin{bmatrix} 0 & b_L \end{bmatrix}}_{D_{kuy}} \begin{bmatrix} y \\ 1 \end{bmatrix}$$

$$w = \phi \left(\underbrace{\begin{bmatrix} 0 \\ W_1 & 0 \\ 0 & W_2 & 0 \\ \vdots & \ddots & \ddots & \ddots \\ 0 & \dots & 0 & W_{L-1} & 0 \end{bmatrix}}_{D_{kvw}} w_k + \underbrace{\begin{bmatrix} W_0 & b_0 \\ 0 & b_1 \\ \vdots & \vdots \\ 0 & b_{L-1} \end{bmatrix}}_{D_{kvy}} \begin{bmatrix} y \\ 1 \end{bmatrix} \right).$$

When $n_k > 0$, the controller has dynamics, making the controller (3) a *recurrent* implicit neural network (RINN). Controllers with memory are useful in applications with partially-observed plants [15]. This model and variations have been used for control in [5]–[8].

C. Problem Statement

We now address the constrained optimization problem:

$$\begin{aligned} \max_K \quad & \mathbb{E} \left[\int_0^T r(x_p(t), u(t)) dt \right] \\ \text{s.t.} \quad & \mathcal{F}(\tilde{P}_{\Delta_p}, K) \text{ stable } \forall \tilde{P}_{\Delta_p} \in \mathcal{M}_\alpha, \\ & K \text{ is of the form in (3)} \end{aligned} \quad (4)$$

where $\mathcal{F}(\tilde{P}_{\Delta_p}, K)$ denotes the closed-loop of \tilde{P}_{Δ_p} and K , and $r : \mathbb{R}^{n_p} \times \mathbb{R}^{n_u} \rightarrow \mathbb{R}$ is the reward function. The integral of the reward over a trajectory on $[0, T]$, where $T \in \mathbb{R}_{\geq 0}$, gives a score to the trajectory. The expectation is taken over a distribution of initial plant states, and any randomness in the training model (for example, disturbances). Note that the simulation model and environment used for rolling out trajectories in training need not be the same as the nominal plant model; it can be a higher-fidelity simulation model.

III. DISK MARGIN CERTIFICATION

In this section, we present a condition certifying that a RINN controller K satisfies the disk margin $D(\alpha, \sigma)$ for a nominal plant P .

A. Transforming Plant Model

We transform the uncertain plant \tilde{P}_{Δ_p} into the form of an LTI system interconnected with an uncertainty block. This form mirrors the form of the RINN controller, and enables the entire closed-loop system to be modeled as an LTI system interconnected with an uncertainty block (grouping the controller's activation functions into the uncertainty block).

We simplify the LTI part of the uncertain plant (2), making an LTI system with inputs w_p and \tilde{u} and outputs v_p and y . Combining $u = v_p + \frac{1-\sigma}{2}w_p$ and $v_p = \tilde{u} + \frac{1+\sigma}{2}w_p$ gives $u = w_p + \tilde{u}$. Plugging this into (1):

$$\begin{aligned} \begin{bmatrix} \dot{x}_p(t) \\ y(t) \end{bmatrix} &= \begin{bmatrix} A_p & B_p \\ C_p & 0 \end{bmatrix} \begin{bmatrix} x_p(t) \\ u(t) \end{bmatrix} \\ &= \begin{bmatrix} A_p & B_p & B_p \\ C_p & 0 & 0 \end{bmatrix} \begin{bmatrix} x_p(t) \\ w_p(t) \\ \tilde{u}(t) \end{bmatrix}. \end{aligned}$$

We next add v_p as an output using $v_p(t)$ from (2):

$$\begin{aligned} \begin{bmatrix} \dot{x}_p(t) \\ v_p(t) \\ y(t) \end{bmatrix} &= \begin{bmatrix} A_p & B_p & B_p \\ 0 & \frac{1+\sigma}{2}I & I \\ C_p & 0 & 0 \end{bmatrix} \begin{bmatrix} x_p(t) \\ w_p(t) \\ \tilde{u}(t) \end{bmatrix} \quad (5) \\ w_p(t) &= \Delta_p(v_p)(t). \end{aligned}$$

Equation (5) gives the plant \tilde{P}_{Δ_p} in the form of an LTI system interconnected with an uncertainty, similar to the controller diagram in Figure 2, as opposed to the structured interconnection in Figure 1.

B. Quadratic Constraints (QCs) on Δ_p and ϕ

With both the plant and the controller now in the form of an LTI system interconnected with an uncertainty or a nonlinearity, we characterize the non-LTI components—that is, Δ_p and ϕ —by describing the relationship between the inputs and outputs of each block with quadratic constraints [16]–[19]. For simplicity and computational tractability, we use static quadratic constraints for both Δ_p and ϕ .

Since Δ_p is diagonal and has \mathcal{L}_2 gain less than or equal to α , it satisfies the following integral quadratic constraint (IQC) for all $\Lambda_p \in \mathbb{R}^{n_u \times n_u}$ where $\Lambda_p \succeq 0$ and diagonal, $v_p \in \mathcal{L}_{2e}^{n_u}$, $w_p = \Delta_p(v_p)$, and $T \geq 0$ [16]:

$$\int_0^T \begin{bmatrix} v_p(t) \\ w_p(t) \end{bmatrix}^\top \begin{bmatrix} \alpha^2 \Lambda_p & 0 \\ 0 & -\Lambda_p \end{bmatrix} \begin{bmatrix} v_p(t) \\ w_p(t) \end{bmatrix} \geq 0. \quad (6)$$

To restrict Δ_p to be LTI, one can include dynamic filters into (6). The class of filters for uncertain LTI dynamics is described in [16].

Since ϕ is applied elementwise and sector-bounded in $[0, 1]$, it satisfies the following quadratic constraint for all $\Lambda_k \in \mathbb{R}^{n_\phi \times n_\phi}$ where $\Lambda_k \succeq 0$ and diagonal, $v_k \in \mathbb{R}^{n_\phi}$, and $w_k = \phi(v_k)$ [20]:

$$\begin{bmatrix} v_k \\ w_k \end{bmatrix}^\top \begin{bmatrix} 0 & \Lambda_k \\ \Lambda_k & -2\Lambda_k \end{bmatrix} \begin{bmatrix} v_k \\ w_k \end{bmatrix} \geq 0. \quad (7)$$

C. Stability Condition

We form the closed-loop system of (5) and (3):

$$\begin{aligned} \begin{bmatrix} \dot{x}(t) \\ v(t) \end{bmatrix} &= \begin{bmatrix} A & B_w \\ C_v & D_{vw} \end{bmatrix} \begin{bmatrix} x(t) \\ w(t) \end{bmatrix} \quad (8) \\ w(t) &= \Delta(v)(t), \end{aligned}$$

where $x(t) = [x_p(t)^\top \ x_k(t)^\top]^\top$, $v(t) = [v_p(t)^\top \ v_k(t)^\top]^\top$, $w(t) = [w_p(t)^\top \ w_k(t)^\top]^\top$, and $\Delta : v \mapsto [\Delta_p(v_p)^\top \ \phi(v_k)^\top]^\top$. The expansions of A, B_w, C_v, D_{vw} matrices are:

$$\begin{aligned} A &= \begin{bmatrix} A_p + B_p D_{kuy} C_p & B_p C_{ku} \\ B_{ky} C_p & A_k \end{bmatrix} & B_w &= \begin{bmatrix} B_p & B_p D_{kuw} \\ 0 & B_{kw} \end{bmatrix} \\ C_v &= \begin{bmatrix} D_{kuy} C_p & C_{ku} \\ D_{kvy} C_p & C_{kv} \end{bmatrix} & D_{vw} &= \begin{bmatrix} \frac{1+\sigma}{2}I & D_{kvw} \\ 0 & D_{kvw} \end{bmatrix}. \end{aligned}$$

Since Δ is formed by stacking Δ_p and ϕ , it satisfies an integral quadratic constraint formed by interleaving the IQCs satisfied by Δ_p and Δ_k : for all $\Lambda_p \succeq 0$ and diagonal, $\Lambda_k \succeq 0$ and diagonal, $v \in \mathcal{L}_{2e}$, $w = \Delta(v)$, and $T \geq 0$,

$$\int_0^T \begin{bmatrix} v(t) \\ w(t) \end{bmatrix}^\top M \begin{bmatrix} v(t) \\ w(t) \end{bmatrix} \geq 0 \quad (9)$$

where

$$M \triangleq \begin{bmatrix} M_{vv} & M_{vw} \\ M_{vw}^\top & M_{ww} \end{bmatrix} = \left[\begin{array}{cc|cc} \alpha^2 \Lambda_p & 0 & 0 & 0 \\ 0 & 0 & 0 & \Lambda_k \\ \hline 0 & 0 & -\Lambda_p & 0 \\ 0 & \Lambda_k & 0 & -2\Lambda_k \end{array} \right].$$

We now present the stability condition for the closed-loop system (8).

Lemma 3.1: Let $\alpha \geq 0$, $\sigma \in \mathbb{R}$, the plant in (1), and the controller in (3) be given. If there exist $X \in \mathbb{R}^{(n_p+n_k) \times (n_p+n_k)}$ with $X \succ 0$, $\Lambda_p \in \mathbb{R}^{n_u \times n_u}$ with $\Lambda_p \succeq 0$ and diagonal, and $\Lambda_k \in \mathbb{R}^{n_\phi \times n_\phi}$ with $\Lambda_k \succeq 0$ and diagonal, such that

$$\begin{bmatrix} A^\top X + XA & XB_w \\ B_w^\top X & 0 \end{bmatrix} + (\star)^\top M \begin{bmatrix} C_v & D_{vw} \\ 0 & I \end{bmatrix} \preceq 0, \quad (10)$$

then the controller satisfies the disk margin $D(\alpha, \sigma)$.

Proof: Since the closed-loop system is in the form of an LTI system interconnected with an uncertainty described by an integral quadratic constraint, we apply Lemma 1 of [8]. ■

Remark 1: This condition can also be used to find the largest α the closed-loop system satisfies by bisection on α .

IV. NEURAL NETWORK TRAINING

To synthesize a neural network controller that satisfies a specified disk margin $D(\alpha, \sigma)$, we use a reinforcement learning procedure that alternates between a training step and a stability margin-enforcing step. The training step improves the controller's performance on the reward function, but the new controller does not necessarily satisfy the desired disk margin. Therefore, we follow the training step with a stability margin-enforcing step that projects the controller into the set of controllers guaranteed to robustly stabilize the plant.

A direct application of Lemma 3.1 gives the following projection problem, with θ' being the controller parameters we would like to project into the set of controller parameters that satisfy the robust stability condition:

$$\begin{aligned} \min_{\theta, X, \Lambda_p, \Lambda_k} \quad & \|\theta' - \theta\| \\ \text{s.t.} \quad & X \succ 0, \Lambda_p \succeq 0, \Lambda_k \succeq 0 \\ & \Lambda_p \text{ and } \Lambda_k \text{ diagonal} \\ & (10) \text{ holds with } \theta. \end{aligned}$$

However, this is not computationally tractable since it is not convex in θ, X, Λ_p , and Λ_k . This is due to bilinear terms in θ and X that appear in (10) (for example, in $A^\top X$) and due to quadratic terms in θ and Λ_p and in θ and Λ_k . Therefore, if using Lemma 3.1 directly, we would project θ' into the following set parameterized by X, Λ_p , and Λ_k :

$$\Theta(X, \Lambda_p, \Lambda_k) \triangleq \{\theta \mid (10) \text{ holds}\}. \quad (12)$$

To reduce conservatism, we leverage the transformation procedure from [8]. Below we provide the resulting matrix inequality that is equivalent to Lemma 3.1 when $\Lambda_k \succ 0$ but jointly convex in θ, X , and Λ_k —leaving only Λ_p fixed during the projection step. For simplicity, we assume the order of the controller is the same as the order of the plant.

Lemma 4.1: Let the disk margin $D(\alpha, \sigma)$, the plant in (1), and $\Lambda_p = \tilde{L}_{\Delta_p}^\top \tilde{L}_{\Delta_p}$, where $\Lambda_p \succeq 0$ and diagonal, be given. If there exist $\hat{\theta} = \{S, R, N_A, N_B, N_C, D_{kuw}, \hat{D}_{kvy}, \hat{D}_{kvw}, \Lambda_k\}$ where

$S \succ 0, R \succ 0, \Lambda_k \succ 0$ and diagonal, and $\begin{bmatrix} R & I \\ I & S \end{bmatrix} \succ 0$ such that (11) holds, then a controller θ can be reconstructed from $\hat{\theta}$ such that the controller satisfies the specified disk margin.

We label the set of $\hat{\theta}$ that satisfy the conditions of Lemma 4.1 for a particular Λ_p as $\hat{\Theta}(\Lambda_p)$. Given $\hat{\theta} \in \hat{\Theta}(\Lambda_p)$, the controller θ can be reconstructed by solving the following for $A_k, B_{kw}, B_{ky}, C_{kv}, D_{kvw}, D_{kvy}, C_{ku}, D_{kuy}$, where U and V are such that $VU^\top = I - RS$ (for example, by taking the SVD):

$$\begin{aligned} N_A &= \begin{bmatrix} SA_p R & 0 \\ 0 & 0 \end{bmatrix} \\ &+ \begin{bmatrix} U & SB_p \\ 0 & I \end{bmatrix} \begin{bmatrix} A_k & B_{ky} \\ C_{ku} & D_{kuy} \end{bmatrix} \begin{bmatrix} V^\top & 0 \\ C_{py} R & I \end{bmatrix} \\ N_B &= SB_p D_{kuw} + UB_{kw} \\ N_C &= \Lambda_k D_{kvy} C_{pv} R + \Lambda_k C_{kv} V^\top \\ \hat{D}_{kvy} &= \Lambda_k D_{kvy}, \quad \hat{D}_{kvw} = \Lambda_k D_{kvw}. \end{aligned}$$

This controller is certified by the given Λ_p , the Λ_k decision variable, and the following construction for X :

$$X \triangleq \begin{bmatrix} I & S \\ 0 & U^\top \end{bmatrix} \begin{bmatrix} R & I \\ V^\top & 0 \end{bmatrix}^{-1}.$$

Therefore, satisfaction of Lemma 4.1 implies $\Theta(X, \Lambda_p, \Lambda_k)$ is nonempty for the above X, Λ_p , and Λ_k .

Note that the transformation between $\hat{\theta}$ and θ also works in the reverse: a $\hat{\theta}$ can be constructed from a θ, X, Λ_p , and Λ_k using the above equations.

Critically, all matrix inequalities in Lemma 4.1 are affine in $\hat{\theta}$, so these conditions can be incorporated into the following semidefinite program for projection:

$$\begin{aligned} \min_{\hat{\theta}} \quad & \|\hat{\theta}' - \hat{\theta}\| \\ \text{s.t.} \quad & S \succ 0, R \succ 0, \Lambda_k \succ 0, \begin{bmatrix} R & I \\ I & S \end{bmatrix} \succ 0 \\ & \Lambda_k \text{ diagonal} \\ & (11) \text{ holds.} \end{aligned} \quad (13)$$

With the above methods to certify a disk margin, to construct $\hat{\theta}$, and to project a $\hat{\theta}$ into $\hat{\Theta}(\Lambda_p)$, we introduce the following training algorithm.

Algorithm 1 alternates between improving the controller through reinforcement learning, and modifying the controller to ensure that the controller satisfies the specified disk margins. While a direct application of the projection in (13) fixes Λ_p , we introduce alternation on Λ_p during training by, in line 5, certifying the disk margin if possible. This both allows Λ_p to vary, and avoids the more expensive projection procedure when possible. If the controller after the training step cannot be certified to satisfy the disk margin, we use the most recent X and Λ_k to transform it into the $\hat{\theta}$ -space. Then, we leverage the projection in (13) to construct \hat{X} and $\hat{\Lambda}_k$ such that $\Theta(\hat{X}, \hat{\Lambda}_p, \hat{\Lambda}_k)$ is nonempty. Finally, we project θ' into this set. We use this projection in θ -space instead of directly transforming the projected $\hat{\theta}$ into a θ since our goal is to find the closest $\theta \in \Theta(X, \Lambda_p, \Lambda_k)$ to θ' , and the procedure to recover θ from $\hat{\theta}$ gives only *some* $\theta \in \Theta(X, \Lambda_p, \Lambda_k)$.

$$\begin{bmatrix} \text{He}(A_p R + B_p N_{A21}) & A_p + B_p N_{A22} C_p + N_{A11}^\top & B_p & B_p D_{kuw} + N_C^\top & \alpha N_{A21}^\top \tilde{L}_{\Delta_p}^\top \\ N_{A11} + A_p^\top + C_p^\top N_{A22}^\top B_p^\top & \text{He}(S A_p + N_{A12} C_p) & S B_p & N_B + C_p^\top \hat{D}_{kvy} & \alpha C_p^\top N_{A22}^\top \tilde{L}_{\Delta_p}^\top \\ \hline B_p^\top & B_p^\top S & -\Lambda_p & 0 & \frac{\alpha(1+\sigma)}{2} \tilde{L}_{\Delta_p}^\top \\ D_{kuw}^\top B_p^\top + N_C & N_B^\top + \hat{D}_{kvy}^\top C_p & 0 & \hat{D}_{kvw} + \hat{D}_{kvw}^\top - 2\Lambda_k & \alpha D_{kuw}^\top \tilde{L}_{\Delta_p}^\top \\ \hline \alpha \tilde{L}_{\Delta_p} N_{A21} & \alpha \tilde{L}_{\Delta_p} N_{A22} C_p & \frac{\alpha(1+\sigma)}{2} \tilde{L}_{\Delta_p} & \alpha \tilde{L}_{\Delta_p} D_{kuw} & -I \end{bmatrix} \preceq 0 \quad (11)$$

Algorithm 1 Neural Network Controller Training

- 1: $\theta \leftarrow$ arbitrary
 - 2: $X, \Lambda_p, \Lambda_k \leftarrow I$
 - 3: **for** $i = 1, \dots, \text{do}$
 - ▷ Reinforcement learning step ◁
 - 4: $\theta' \leftarrow \text{REINFORCEMENTLEARNINGSTEP}(\theta)$
 - ▷ Robust stability-enforcing step ◁
 - 5: **if** $\exists X', \Lambda'_p, \Lambda'_k : \theta'$ satisfies disk margins **then**
 - 6: $\theta, X, \Lambda_p, \Lambda_k \leftarrow \theta', X', \Lambda'_p, \Lambda'_k$
 - 7: **else**
 - 8: $\hat{\theta}' \leftarrow \text{CONSTRUCTTHETAHAT}(\theta', X, \Lambda_k)$
 - 9: $\hat{\theta} \leftarrow \text{THETAHATPROJECT}(\hat{\theta}', \hat{\Theta}(\Lambda_p))$
 - 10: $X, \Lambda_k \leftarrow \text{EXTRACTFROM}(\hat{\theta})$
 - 11: $\theta \leftarrow \arg \min_{\theta} \|\theta - \theta'\| : \theta \in \Theta(X, \Lambda_p, \Lambda_k)$
 - 12: **end if**
 - 13: **end for**
-

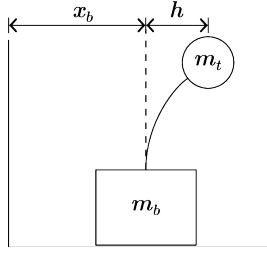


Fig. 3. Diagram of the flexible rod on a cart.

Remark 2: One useful choice for initializing parameters θ , X , and Λ_p in Algorithm 1 is an LTI controller synthesized to stabilize, or robustly stabilize, the plant.

V. NUMERICAL EXPERIMENTS

We demonstrate the performance of our method through simulation on a flexible rod on a cart. We compare our method with two unconstrained neural network controllers and an LTI controller. For shorthand, we refer to our method as Stability Margin Recurrent Implicit Neural Network (SM-RINN). The unconstrained neural network controllers we compare against are an unconstrained RINN (U-RINN) and a standard fully connected feedforward neural network (FCNN). The LTI controller (referred to as LTI) is trained using the same method as the SM-RINN: it guarantees the same stability margins.

Since all plants and controller models are defined in continuous time, we implement them by simulating between timesteps with the Runge-Kutta 4th order method. We use PyTorch and Ray RLLib with the proximal policy

optimization algorithm for training. All code is online at github.com/neelayjunnarkar/nn-stability-margins.

The full model of the flexible rod on a cart is as follows:

$$\begin{aligned} \dot{x}_f(t) &= \begin{bmatrix} 0 & I \\ -M^{-1}K & -M^{-1}B \end{bmatrix} x_f(t) + \begin{bmatrix} 0 \\ M^{-1} \begin{bmatrix} 1 \\ 0 \end{bmatrix} \end{bmatrix} u(t) \\ y(t) &= \begin{bmatrix} 1 & 1 & 0 & 0 \end{bmatrix} x_f(t) \\ M &= \begin{bmatrix} m_b + m_r + \rho L & m_t + \frac{\rho L}{3} \\ m_t + \frac{\rho L}{3} & m_t + \frac{\rho L}{5} \end{bmatrix} \\ K &= \begin{bmatrix} 0 & 0 \\ 0 & \frac{4EI}{L^3} \end{bmatrix}, \quad B = \begin{bmatrix} 0 & 0 \\ 0 & 0.9 \end{bmatrix} \end{aligned} \quad (14)$$

where $x_f(t) = [x_b(t) \ h(t) \ \dot{x}_b(t) \ \dot{h}(t)]^\top \in \mathbb{R}^4$ is the state of the flexible rod on a cart, $x_b(t)$ is the position of the rod's base, $h(t)$ is the horizontal deviation of the top of the rod from the base, $m_b = 1$ kg is the mass of the base, $m_t = 0.1$ kg is the mass of an object at the top of the rod, $L = 1$ m is the rod length, $\rho = 0.1$ N/m is the mass density of the rod, $r = 10^{-2}$ m is the radius of the rod cross-section, $E = 200 \cdot 10^9$ GPa is the Young's modulus of steel, and $I = \frac{\pi}{4} r^4$ m⁴ is the area second moment of inertia. The output y represents the measurement of the position of the rod tip.

The flexible model is used in simulation for training. As a demonstration of using a simpler model for design, we use the following rigid model of the rod on a cart for all stability margin properties of the SM-RINN and LTI controllers:

$$\begin{aligned} \dot{x}_r(t) &= \begin{bmatrix} 0 & 1 \\ 0 & 0 \end{bmatrix} x_r(t) + \begin{bmatrix} 0 \\ \frac{1}{m_b + m_r + \rho L} \end{bmatrix} u(t) \\ y(t) &= x_b(t) \end{aligned} \quad (15)$$

where $x_r(t) = [x_b(t) \ \dot{x}_b(t)]^\top$. For the SM-RINN and LTI controllers, we impose a requirement that they satisfy a disk margin with $\alpha = 0.353$ and $\sigma = 0$. The value of α can be tuned to tradeoff between reward and robustness. This particular disk margin implies a lower bound on the gain margin of 3dB and a lower bound on the phase margin of 20°. Note that disk margins ensure robustness to simultaneous variation in gain and phase as well, which gain and phase margins do not consider.

We simulate the controllers and plant with a time step of 0.001 seconds, and train with a time horizon of 2 seconds. The reward for each time step is $\exp(-\|x_f(t)\|^2) + \exp(-u(t)^2)$. Initial conditions are sampled uniformly at random with $x_b(0) \in [-1, 1]$ m, $h(0) \in [-0.44, 0.44]$ m, $\dot{x}_b(0) \in [-0.25, 0.25]$ m/s, and $\dot{h}(0) \in [-2, 2]$ m/s. The control input is saturated to the interval $[-20, 20]$ N.

For the two RINN controllers, we use a state size of 2 ($n_k = 2$) and 16 activation functions ($n_\phi = 16$). For the FCNN, we use two layers of size 19 each to match the total

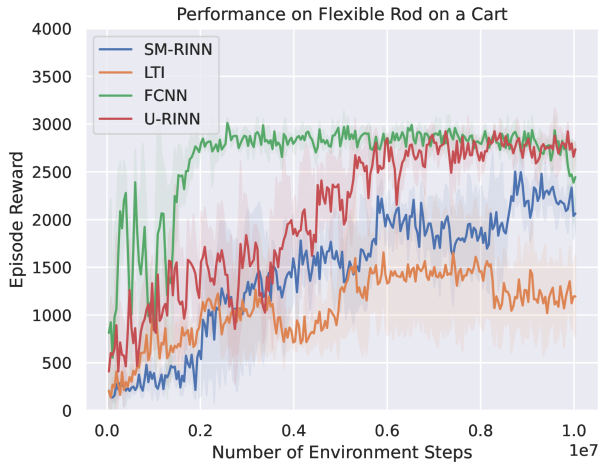


Fig. 4. Evaluation reward vs. number of training environment steps for the Stability Margin Recurrent Implicit Neural Network (SM-RINN, our method), Fully Connected Neural Network (FCNN), Unconstrained RINN (U-RINN), and linear time-invariant (LTI) controllers on the flexible rod on a cart. The SM-RINN and LTI controllers both guarantee a disk margin of $\alpha = 0.353$ with skew $\sigma = 0$. The solid line represents the mean, and the shaded region represents 1 standard deviation. The reward is upper bounded by 4000, and lower bounded by 0. Higher reward indicates a combination of lower control effort and smaller state of the flexible rod on a cart.

number parameters of the RINN controllers. The U-RINN, FCNN, and LTI controllers are trained with a learning rate of 10^{-4} . The SM-RINN is trained with a learning rate of $5 \cdot 10^{-5}$ to alleviate instability. The activation function is \tanh for all neural network controllers.

Figure 4 shows reward vs. number of training environment steps sampled, with mean and standard deviations taken over three runs of each controller. The two controllers with the highest rewards are the unconstrained controllers (FCNN and U-RINN, both about 3000). The next highest is the SM-RINN (reward about 2250), which guarantees stability margins. The LTI controller, which guarantees the same stability margins as the SM-RINN, achieves the lowest reward (about 1500). This ordering shows a typical performance vs. robustness tradeoff: the methods without robustness requirements achieve the highest reward. Note that our method, the SM-RINN, achieves a significant reward improvement over the LTI controller while guaranteeing the same margin.

VI. CONCLUSION

We presented a method to analyze the disk margin of a neural network controller, and a method to train a neural network controller to maximize reward subject to it satisfying a specified disk margin. We demonstrated our approach on a flexible rod on a cart, where it achieved significantly higher reward than did an LTI controller. Our method enables neural networks to be used as controllers in safety-critical applications where stability margins are required.

REFERENCES

[1] *Code of Federal Regulations. Title 14: Chapter 1: Subchapter C: Part 25: Airworthiness standards: Transport category airplanes*, 2023.

[2] H. Yin, P. Seiler, and M. Arcak, “Stability Analysis Using Quadratic Constraints for Systems With Neural Network Controllers,” *IEEE Transactions on Automatic Control*, vol. 67, no. 4, Apr. 2022.

[3] N. Hashemi, J. Ruths, and M. Fazlyab, “Certifying Incremental Quadratic Constraints for Neural Networks via Convex Optimization,” in *Proceedings of the 3rd Conference on Learning for Dynamics and Control*, PMLR, May 29, 2021.

[4] P. Pauli, D. Gramlich, J. Berberich, and F. Allgöwer, “Linear Systems with Neural Network Nonlinearities: Improved Stability Analysis via Acausal Zames-Falb Multipliers,” in *2021 60th IEEE Conf. on Decision and Control (CDC)*, Dec. 2021.

[5] F. Gu, H. Yin, L. E. Ghaoui, M. Arcak, P. Seiler, and M. Jin, “Recurrent Neural Network Controllers Synthesis with Stability Guarantees for Partially Observed Systems,” *Proceedings of the AAAI Conference on Artificial Intelligence*, Jun. 2022.

[6] R. Wang, N. H. Barbara, M. Revay, and I. R. Manchester, “Learning Over All Stabilizing Nonlinear Controllers for a Partially-Observed Linear System,” *IEEE Control Systems Letters*, vol. 7, 2023.

[7] N. Junnarkar, H. Yin, F. Gu, M. Arcak, and P. Seiler, “Synthesis of Stabilizing Recurrent Equilibrium Network Controllers,” in *2022 IEEE 61st Conference on Decision and Control (CDC)*, Dec. 2022.

[8] N. Junnarkar, M. Arcak, and P. Seiler, *Synthesizing Neural Network Controllers with Closed-Loop Dissipativity Guarantees*, 2024. arXiv: 2404.07373 [eess.SY].

[9] N. Barabanov and D. Prokhorov, “Stability analysis of discrete-time recurrent neural networks,” *IEEE Transactions on Neural Networks*, vol. 13, no. 2, pp. 292–303, Mar. 2002.

[10] E. Sontag, “Recurrent Neural Networks: Some Systems-Theoretic Aspects,” in *Dealing with Complexity: A Neural Networks Approach*, London: Springer, 1998.

[11] K. Zhou, J. C. Doyle, and K. Glover, *Robust and Optimal Control*. USA: Prentice-Hall, Inc., 1996.

[12] P. Seiler, A. Packard, and P. Gahinet, “An Introduction to Disk Margins [Lecture Notes],” *IEEE Control Systems Magazine*, vol. 40, no. 5, Oct. 2020.

[13] A.-K. Schug, P. Seiler, and H. Pfifer, “Robustness Margins for Linear Parameter Varying Systems,” *AerospaceLab Journal*, vol. Issue 13, 2017.

[14] L. El Ghaoui, F. Gu, B. Travacca, A. Askari, and A. Tsai, “Implicit Deep Learning,” *SIAM Journal on Mathematics of Data Science*, vol. 3, no. 3, Jan. 2021.

[15] F. M. Callier and C. A. Desoer, *Linear System Theory* (Springer Texts in Electrical Engineering), J. B. Thomas, red. New York, NY: Springer, 1991.

[16] A. Megretski and A. Rantzer, “System Analysis Via Integral Quadratic Constraints,” *IEEE Transactions on Automatic Control*, vol. 42, no. 6, Jun. 1997.

[17] P. Seiler, “Stability Analysis With Dissipation Inequalities and Integral Quadratic Constraints,” *IEEE Transactions on Automatic Control*, vol. 60, no. 6, Jun. 2015.

[18] C. W. Scherer, “Dissipativity and Integral Quadratic Constraints: Tailored Computational Robustness Tests for Complex Interconnections,” *IEEE Control Systems Magazine*, vol. 42, no. 3, pp. 115–139, Jun. 2022.

[19] J. Veenman and C. W. Scherer, “IQC-synthesis with General Dynamic Multipliers,” *International Journal of Robust and Nonlinear Control*, vol. 24, no. 17, Nov. 25, 2014.

[20] M. Fazlyab, M. Morari, and G. J. Pappas, “Safety Verification and Robustness Analysis of Neural Networks via Quadratic Constraints and Semidefinite Programming,” *IEEE Transactions on Automatic Control*, vol. 67, no. 1, Jan. 2022.